Multilayer volume holographic optical memory

Vladimir Markov, James Millerd, James Trolinger, and Mark Norrie

MetroLaser Inc., Suite 100, Skypark Circle 18010, Irvine, California 92614

John Downie and Dogan Timucin

NASA Ames Research Center, M/S 269-3, Moffett Field, California 94035

Received October 2, 1998

We demonstrate a scheme for volume holographic storage based on the features of shift selectivity of a speckle reference-wave hologram. The proposed recording method permits more-efficient use of the recording medium and yields greater storage density than spherical or plane-wave reference beams. Experimental results of multiple hologram storage and replay in a photorefractive crystal of iron-doped lithium niobate are presented. The mechanisms of lateral and longitudinal shift selectivity are described theoretically and shown to agree with experimental measurements. © 1999 Optical Society of America

OCIS codes: 210.0210, 090.0090, 210.2860, 030.6140, 090.4220.

Holographic memory has been a subject of interest for decades since it was suggested by van Heerden.[1] High information density, parallel access, and high-speed retrieval are among the features that make this technique of data storage so attractive. Selective properties of volume holograms that are due to angular[2,3] or wavelength[4] deviation from the Bragg condition as well as to reference-beam phase encoding[5,6] are methods that are frequently used for data input and retrieval. The combination of reference-beam phase encoding with spatial-shift multiplexing was shown to be an efficient approach for high-density holographic information storage.[7,8] A similar technique that uses a reference beam comprising many plane waves (or a spherical wave) was suggested and experimentally demonstrated.[9] Although all these methods permit high-density storage of the holograms, the longitudinal shift component of the volume recording medium has not been considered for coding the individual pages of information. Recently a method of multilayer optical storage was discussed in which information is recorded at different depths within the medium, similar to that of a magnetic-disk stack currently used in PC's.[10,11] It was demonstrated that holograms can be recorded as thin layers within the volume of the medium to provide large information storage capacity and fast data transfer rates.[12] In this Letter we discuss and demonstrate a single-volume, multilayer holographic optical memory based on the features of three-dimensional spatial-shift selectivity in a volume hologram recorded with a speckle-encoded reference beam (SRB).

For our analysis we consider the case in which the hologram is recorded by a plane-wave signal beam $S_o(r)$ and a SRB $R_o(r)$ with a divergence angle $\delta\theta_{\mathrm{SP}}$, as shown in Fig. 1. The two recording beams intersect at an angle θ_0, forming an interference pattern with a grating spacing $\Lambda = \lambda/\sin(\theta_0)$, assuming a SRB incidence angle $\theta_{R_o} = 0$. It was shown[13] that, in the first Born approximation, the diffracted wave amplitude $S(r)$, when it is reconstructed with a SRB that is different from the recording beam [i.e., $R(r) \neq R_o(r)$], can be described as

$$S(r) = k_o^2 \iiint_V \delta\varepsilon(r')R(r')\,\frac{\exp[ik_o(r - r')]}{4\pi|r - r'|}\,\mathrm{d}^3r' \,. \tag{1}$$

Here $\delta\varepsilon(r')$ is the modulated component of the recording medium's permittivity $\delta\varepsilon(r) \propto S_o(r)R_o{}^*(r)$ and V is the volume of the hologram. Equation (1) is valid if the hologram is a volume hologram and its thickness T exceeds the longitudinal speckle size, i.e., $T \gg \lambda/(\delta\theta_{\mathrm{SP}})^2 \gg \lambda/2\theta_o$. Then, by assuming a plane-wave signal beam $S_o(r) = \exp(ik_{\mathrm{os}}r)$ and a reconstructed signal beam $S(r)$ propagating in the same direction, we can reduce Eq. (1) to

$$S(r) = \exp(ik_{\mathrm{os}}r) \iiint_V C(r, r')\,\mathrm{d}^3r' \,. \tag{2}$$

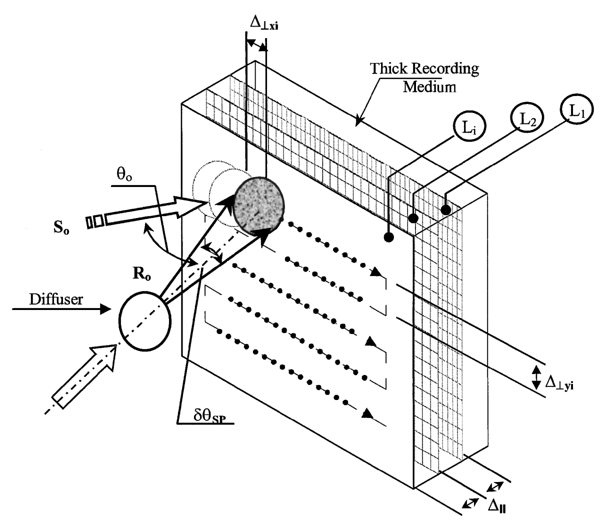

Fig. 1. Schematic of multilayer speckle–reference-beam-encoded hologram recording. Abbreviations are defined in text.

0146-9592/99/040265-03$15.00/0

It is assumed here that the speckle pattern intensity distribution has Gaussian statistics and that its spatial autocorrelation function $C(r, r')$ is determined by mutual intensity of the recording and reconstructing SRB's,[14] i.e., $C(r, r') = \langle R_o^*(r) R(r') \rangle$.

Contrary to the usual practice for a phase-encoded holographic memory, we consider the case when the spatial amplitude–phase distribution of reconstruction beam $R(r)$ remains identical to that of recording beam $R_o(r)$. The difference between $R(r)$ and $R_o(r)$ is due to the mutual spatial shift of the hologram and the reconstructing beam, i.e., $R(r) = R_o(r + \mathbf{\Delta})$, where $\mathbf{\Delta} = \Delta_\perp \hat{q} + \Delta_\| \hat{Z}$, $\Delta_\perp$ and Δ_Π are transverse and longitudinal components of the shift, respectively, and $\hat{q}$ and $\hat{z}$ are unity vectors in the same directions.

As the experimentally measured value is the diffracted beam intensity $I_D = |S|^2$, it is convenient to introduce the parameter of relative diffracted beam intensity $I_{DN}(\Delta) = I_D(\Delta)/I_{D(\Delta=0)}$, where the measured diffracted intensity $I_D(\Delta)$ is normalized by its peak value at zero shift, $I_{D(\Delta=0)}$. By incorporating the three-dimensional correlation function $C(r, r')$ derived in Ref. 13 and using the Fresnel–Kirchhoff diffraction integral, we can express the dependence $I_{DN}(\mathbf{\Delta}_\perp)$ as

$$I_{DN}(\Delta_\perp) = \frac{I_D(\Delta_\perp)}{I_{D(\Delta_\perp=0)}}$$

$$= \frac{\left| \int_0^T \exp\left(\frac{i k_o n \Delta_\perp^2}{2 d_{\mathrm{dh}}}\right) \int_{-\infty}^{+\infty} \int |K_D(\mathbf{q})|^2 \exp\left(-\frac{i k_o n}{d_{\mathrm{dh}}} \mathbf{q} \mathbf{\Delta}_\perp\right) \mathrm{d}^2 q \, \mathrm{d}z \right|^2}{T^2 \int_{-\infty}^{+\infty} \int |K_D(\mathbf{q})|^2 \, \mathrm{d}^2 q}, \tag{3}$$

here $K_D(\mathbf{q})$ is the diffuser aperture function, $k_o = 2\pi/\lambda$, $\mathbf{q} = q_x \mathbf{x} + q_y \mathbf{y}$, n is refractive index of the recording medium, and d_{dh} is the diffuser–hologram distance.

It follows from Eq. (3) that any lateral mismatch between the hologram and reconstruction beam $R(r)$ leads to a decrease in the intensity of the diffracted beam. Figure 2 shows the falloff in $I_{DN}(\Delta)$ that occurs for lateral shift ($\Delta_\| =$ constant). One of the important features of this type of selectivity is that no ripples are observed as a function of spatial mismatch, unlike in the case of angular or spectral selectivity of volume holograms recorded with plane or spherical waves. The monotonic decrease in diffraction efficiency as a function of shift distance results in much less cross talk between stored images than can be obtained by use of other forms of multiplexing. Furthermore, the spatial decorrelation is symmetric within the plane perpendicular to the Z direction, whereas other forms of multiplexing have high selectivity only in the dispersion plane.

Because the speckle pattern has a three-dimensional nature, the longitudinal shift also results in spatial decorrelation between the hologram and the reconstructing speckle beam, and thus a third dimension can be used to multiplex information. It can be shown that, analogously to $I_{DN}(\Delta_\perp)$, the diffracted beam intensity $I_{DN}(\Delta_\|) \rightarrow 0$ when the shift distance $\Delta_\|$ exceeds the longitudinal correlation length $\langle \sigma_\| \rangle$ (see Fig. 2). The longitudinal shift selectivity opens the possibility of implementing several virtual layers of holograms within the same volume of the recording medium.

SRB holograms were recorded in 2.8-mm-thick $Fe:LiNbO_3$ (0.02% Fe/mol) crystal by three-dimensional multiplexing. The crystal, with its C axis lying in the plane of the recording beams, was set onto an XYZ computer-controlled positioning table, which had a precision of 0.025 μm in the X, Y, and Z planes. A 1-cm-diameter cw argon laser beam ($\lambda = 515$ nm, $P = 40$ mW/cm^2) was used as the coherent light source for hologram recording. The SRB had a lateral speckle size $\langle \sigma_\perp \rangle \approx 3$ μm and intersected the plane-wave signal beam at an angle of $\theta_0 = 35°$ ($\theta_{R_o} = 0°$ and $\theta_{S_o} = 35°$). The diffracted beam intensity was measured with a p–i–n photodetector.

The diffraction efficiency of the hologram in its original position ($\Delta = 0$) was approximately 10^{-3}. After each hologram was recorded, a lateral shift of $\Delta_\perp = 10$ μm was introduced to record the next page of information. The raster scan sequence was used to multiplex images in X, Y, and Z, as shown in Fig. 1. During reconstruction, proper mutual repositioning of the hologram and the SRB resulted in information retrieval. A typical sequence of 30 holograms stored in the form of a 6×5 matrix is shown in Fig. 3. The scan step length for this matrix reconstruction was 0.25 μm. Notice the symmetric nature of the selectivity in both the X and the Y directions that is characteristic of use of a SRB.

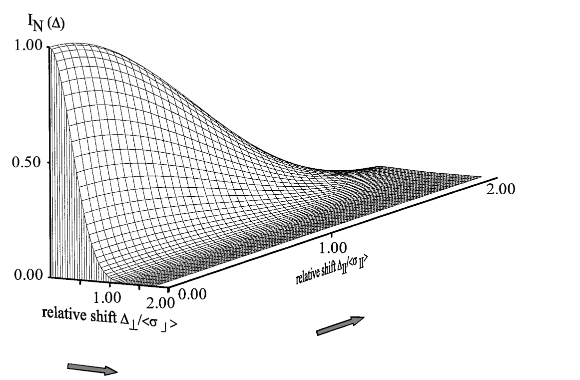

Fig. 2. Calculated diffracted beam intensity $I_N(\Delta)$ as a function of lateral $\Delta_\perp$ and longitudinal $\Delta_\|$ shifts for a hologram recorded and reconstructed with a speckle-encoded reference beam.

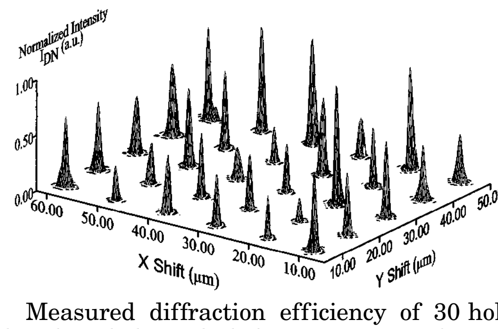

Fig. 3. Measured diffraction efficiency of 30 holograms multiplexed with lateral shift $\Delta_\perp = 10$ μm between successive recordings.

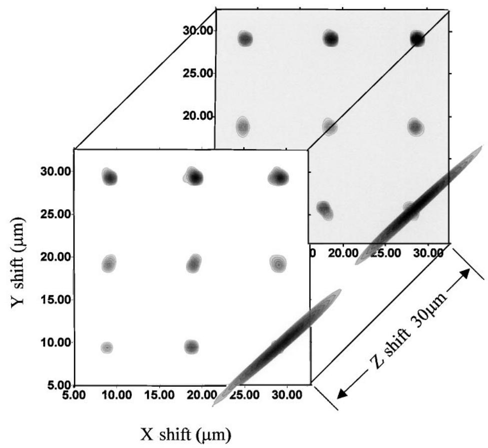

Fig. 4. Measured diffracted beam intensity as a function of spatial shift in the X, Y, and Z directions for two layers of holographic recordings that have a longitudinal shift of 30 μm between layers. Each layer is composed of a 3×3 matrix of holograms. The contour lines correspond to 7% increments normalized to the largest measured intensity. For clarity, the Z dependence for only two of the holograms is shown.

Once recording of the first layer, L_1, was completed, we formed the next layer, L_i, by shifting the recording medium (or the diffuser that generated the speckle pattern) along the central axis of the speckle-beam propagation. The shift magnitude, as discussed above, should satisfy the condition that $\Delta_{\parallel} \geq \langle \sigma_{\parallel} \rangle$, which, for our experimental setup, was ~ 30 μm. In this way a new layer, L_2, could be recorded with the same lateral shift selectivity, and thus a new matrix of $n_{L_2} \times m_{L_2}$ holographic pages was formed. The effect of longitudinal shift selectivity was measured for two holograms and is shown in Fig. 4 as a contour plot of diffracted intensity. A longitudinal shift (Z direction) of $\Delta_{\parallel} = 30$ μm was introduced between successive recordings. Figure 4 also shows an example of the diffracted signal reconstructed from a two-layer structure, in which each layer is composed of a 3×3 matrix. These results agree with our analysis and show that use of a speckle-wave reference beam permits holographic shift multiplexing in three spatial dimensions with a selectivity determined by the average transverse and longitudinal speckle size.

We now estimate the storage density for the technique of holographic data multiplexing described above. The number of holograms $N_{\perp}$ to be recorded in one layer can be calculated as the ratio between an effective area F of the recording medium and unitary lateral shift area $(\Delta_{\perp})^2$ in this plane, i.e., $N_{\perp} \approx (l_x \times l_y)/(\Delta_{\perp})^2$, where l_x and l_y are lateral dimensions of the recording medium. The number of available layers is proportional to $T/\Delta_{\parallel}$. The total number of holograms that can be recorded with a shift selectivity scheme can be estimated as $N_{\mathrm{SP}} = V/[(\Delta_{\perp})^2 \times \Delta_{\parallel}]$. This number leads to $N_{\mathrm{SP}} \sim 4 \times 10^9$ holograms for a 1 cm $\times$ 1 cm $\times$ 1 cm crystal for the experimental conditions described above ($\langle \sigma_{\perp} \rangle \approx 3$ μm, $\langle \sigma_{\parallel} \rangle \approx 30$ μm). In a practical system the dynamic range of the refractive-index variation and the signal-to-noise ratio of the reconstructed image further limits the maximum storage density. The average signal-to-noise ratio for each of the holograms reconstructed in these experiments was ≤ 45, measured as the ratio of the Fourier-filtered dc component of the diffracted beam to the collected scattered light that propagates in the same direction. At fixed experimental conditions, such as recording-beam ratio, exposure level, and form of the aperture in the diffuser plane, the value of the signal-to-noise ratio depends on the ratio of the introduced shift $\Delta_{\perp,\parallel}$ to the magnitude of the correlation radius $\langle \sigma_{\perp,\parallel} \rangle$ in the corresponding direction.

In conclusion, we have demonstrated the possibility of creating a multilayer holographic memory in a photorefractive crystal based on the three-dimensional spatial-shift selectivity of speckle-encoded reference waves. The method achieves high-density data storage with a simple storage-retrieval architecture.

This research was supported in part by the NASA Ames Research Center. The authors thank Michael Dang for technical assistance. V. Markov's e-mail address is vmarkov@metrolaserinc.com.

References

1. P. Van Heerden, Appl. Opt. **2,** 156 (1963).
2. F. H. Mok, Opt. Lett. **18,** 915 (1993).
3. S. Tao, D. Selviah, and J. Midwinter, Opt. Lett. **18,** 912 (1993).
4. J. Rosen, M. Segev, and A. Yariv, Opt. Lett. **18,** 744 (1993).
5. G. Rakuljic, V. Leyva, and A. Yariv, Opt. Lett. **17,** 1471 (1992).
6. C. Alves, G. Pauliat, and G. Roosen, Opt. Lett. **19,** 1894 (1994).
7. A. Darskii and V. Markov, Proc. SPIE **1600,** 318 (1992).
8. V. Markov, Yu. Denisyuk, and R. Amezquita, Opt. Mem. Neural Networks **6,** 91 (1997).
9. D. Psaltis, M. Levene, A. Pu, G. Barbastathis, and K. Curtis, Opt. Lett. **20,** 782 (1995).
10. J. Rosen, Proc. SPIE **2514,** 14 (1995).
11. S. Chinn and E. Swanson, Opt. Lett. **21,** 899 (1996).
12. P. Mitkas and L. Irakliotis, Opt. Mem. Neural Networks **3,** 217 (1994).
13. A. Darskii and V. Markov, Opt. Spectrosc. **65,** 661 (1988).
14. L. Leuschacke and M. Kirchner, J. Opt. Soc. Am. A **7,** 827 (1990).